Thermal and electrical resistivities of aluminium below 4.2 K

1993 J. Phys.: Condens. Matter 5 7797

(http://iopscience.iop.org/0953-8984/5/42/003)

J. Phys.: Condens. Matter 5 (1993) 7797–7814. Printed in the UK

Thermal and electrical resistivities of aluminium below 4.2 K

Y Z Hou and J F Kos
Department of Physics, University of Regina, Regina, Saskatchewan, Canada S4S 0A2

Received 8 December 1992, in final form 20 July 1993

Abstract. High-accuracy thermal conductivity measurements were carried out on two samples of pure aluminium below 4.2 K. Along with electrical resistivity measurements on one of the samples and high-accuracy electrical resistivity measurements available in the literature, these results permitted a determination of the electron–electron scattering terms in the thermal and electrical resistivities. The coefficients of these terms are in very good agreement with the values predicted by MacDonald. In addition, the electron–phonon component ρ_{ep} of the electrical resistivity was successfully separated from the component ρ_d due to deviations from Matthiessen's rule.

1. Introduction

After more than a century of experiment and analysis, a detailed understanding of the transport properties of metals is beginning to emerge. Bass *et al* [1] have provided a fascinating review of our present knowledge of the electrical resistivity of the alkali metals, in which most of the various electron-scattering processes are accounted for.

These advances have been due to the development of high-accuracy measuring instruments and subtle theoretical analysis. For metals with non-spherical Fermi surfaces, the problems are more complicated and our knowledge is correspondingly limited. However, aluminium has a cubic structure, which allows some simplification of theoretical calculations, and despite the complexity of its Fermi surface is considered a 'simple metal'. Also, it is available in high purity, can be annealed in air and is easily handled. Consequently, considerable work has been carried out on this metal.

Garland and Bowers [2] found that in aluminium ρ varied approximately as T^2 below 4.2 K and tentatively attributed this term to electron–electron scattering $\rho_{ee} = aT^2$ where $a \simeq 5 \times 10^{-15}$ Ω m K^{-2}. Subsequent theoretical calculations by Lawrence and Wilkins [3] determined $a_{calc} = 0.12 \times 10^{-15}$ Ω m K^{-2}. Furthermore, the calculations by Lawrence and Wilkins [4] provided an expression for the electron–phonon component, $\rho_{ep} = b_{ep}T^5$ where $b_{ep} \simeq 2.0 \times 10^{-16}$ Ω m K^{-5} (as obtained by Ribot *et al* [5] by extrapolating the curves published by Lawrence and Wilkins (figure 1 of reference [4]) to lower temperatures).

An excellent review of the historical background of electron–electron scattering in the electrical resistivity of aluminium is provided in the paper by Ribot *et al* [5] and comprehensive authoritative presentations are offered in the review papers by Kaveh and Wiser [6] and by van Wucht *et al* [7]. This period is capped by the theoretical advances of MacDonald and Geldart [8, 9], which extend the work of Lawrence and Wilkins to incorporate a phonon-mediated contribution to the scattering amplitudes to provide values of $a_{calc} = 4.1 \times 10^{-15}$ Ω m K^{-2} and $A_{calc} = 7.1 \times 10^{-7}$ m W^{-1} where $W_{ee} = A_{calc}T$ is the component of the thermal resistivity due to electron–electron scattering, and by the superlative experimental data of ρ (for $T < 4.2$ K) provided by Ribot *et al* [5].

0953-8984/93/427797+18$07.50

2. Experimental method

A computer-controlled, high-accuracy, low-temperature thermal conductivity apparatus, previously described [10], was used to measure the thermal conductivity K of two samples of aluminium whose characteristics are given in table 1. These samples were obtained from Johnson Matthey Ltd, who provided the following impurity analysis: for Al-1, the purity is 99.999% with 5 ppm Mg and 4 ppm Si; for Al-2, the purity is 99.999% with 6 ppm Mg and 4 ppm Cu.

Table 1. Characteristics of samples.

Sample	Diameter (μm)	Length (mm)	Residual resistivity ρ_0 (10^{-12} Ω m)	Lorenz number L_0 (10^{-8} W Ω K^{-2})
Al-1	503.4 ± 0.5	159.86 ± 0.02	9.731 ± 0.007	2.452 ± 0.009
Al-2	1522.8 ± 0.05	1850.41 ± 0.05	6.31 ± 0.03	2.44 ± 0.02

Sample Al-1 was mounted as obtained from the spool but Al-2 was wound in a spiral on a quartz tube 1.27 cm in diameter and annealed in an oven (in air) for 10 h at 450 °C, then slowly cooled. It was subsequently gently slipped onto a 1.27 cm diameter teflon tube with walls 0.5 mm thick. The windings were spaced with multifilament nylon fishing line before mounting this sample in our apparatus.

Hair-thin slivers of aluminium were cut from the sample, under a microscope, with one end of each sliver still attached to the sample to provide thermal and electrical potential leads (about 2 cm from each end of the sample). The other ends of the slivers were soldered to 0.25 mm diameter high-purity aluminium wires (as shown in figure 1 of reference [10]). These wires provided thermal contacts to the thermometers and electrical contacts to leads from the digital nanovoltmeter. The tiny contacts to the samples allowed accurate measurements of the effective lengths of the samples with a travelling microscope.

The effective length of Al-1 was measured to about two parts in 10^4 and that of Al-2 was measured to about three parts in 10^5. The average cross-sectional areas, and hence the average diameters of the samples, were determined by measuring their actual lengths and weighing them to within about one part in 10^3 for Al-1 and one part in 10^4 for Al-2. The specific gravity of Al = 2.6989 at 20 °C [16] was used to calculate the cross-sectional areas. The room-temperature size factors of the samples were therefore determined to about two parts in 10^4 for Al-2 and one part in 10^3 for Al-1. These values represent numerical averages; the actual sample diameters probably vary along the lengths of the samples by considerably more than one part in 10^3.

The accuracy of the thermal conductivity data depends on the size of the temperature gradient ΔT selected, on the temperature stability attained and on the accuracy of intercalibration of the two thermometers in contact with the potential leads of the sample. Over most of the temperature range a temperature gradient $\Delta T = 0.3$–0.5 K was used; however at the lowest temperatures only a small gradient could be obtained (about 0.1 K at 2.5 K).

Although the absolute temperature scale is reliable to somewhat less than 1 mK in the range of interest, temperatures were read to 0.01 mK, and with proper intercalibration corrections reliable *temperature differences* could be measured to about 0.1 mK.

During the same run in which the K values were obtained and without raising the temperature above 20 K, an intercalibration of thermometers was carried out (with the

sample heater off). These intercalibrations were used to provide corrected values of the thermal conductivity K_c. The upper limit to the relative accuracy of the corrected values of the thermal conductivity K_c was about two parts in 10^4 with $\Delta T \simeq 0.5$ K. The lower limit was about one part in 10^3 for $\Delta T \simeq 0.1$ K. The *absolute accuracy* was limited by the average size factor to be about one part in 10^3 for Al-1.

3. Results and analysis

The corrected values of the thermal conductivity K_c from 2.5 K to 4.2 K for samples Al-1 and Al-2 and the measured values of the electrical resistivity ρ from 2.9 K to 5.9 K for sample Al-1 are listed in tables 2 and 3 respectively. During measurements on Al-2 only a few low-temperature points (ρ, T) were taken (sufficient only to provide a value of ρ_0 by extrapolation to $T = 0$).

Table 2. Corrected values of the thermal conductivity of Al-1 and Al-2 as a function of temperature.

Al-1		Al-2	
T (K)	K_c (10^4 W m^{-1} K^{-1})	T (K)	K_c (10^4 W m^{-1} K^{-1})
2.547	0.6285	2.462	0.9319
2.558	0.6313	2.610	0.9839
2.601	0.6411	2.708	1.0151
2.634	0.6491	2.710	1.0154
2.708	0.6629	2.717	1.0177
2.765	0.6766	2.785	1.0414
2.806	0.6887	2.874	1.0799
2.860	0.7027	2.907	1.0909
2.972	0.7299	2.992	1.1200
3.132	0.7658	3.018	1.1287
3.248	0.7907	3.056	1.1411
3.348	0.8114	3.063	1.1439
3.516	0.8455	3.192	1.1841
3.699	0.8808	3.294	1.2162
3.925	0.9229	3.410	1.2507
4.095	0.9544	3.587	1.3000
4.105	0.9553	3.700	1.3299
		3.865	1.3729
		4.044	1.4161
		4.202	1.4608

The low-temperature thermal resistivity $W = 1/K_c$ and electrical resistivity ρ of aluminium may be written as

$$W = W_0 + W_{ep} + W_d + W_{ee} + W_v + W_m \tag{1}$$

and

$$\rho = \rho_0 + \rho_{ep} + \rho_d + \rho_{ee} + \rho_m \tag{2}$$

Table 3. Raw data of the electrical resistivity of Al-1 as a function of temperature.

T (K)	ρ (10^{-12} Ω m)	T (K)	ρ (10^{-12} Ω m)
2.907	9.771	4.678	9.865
2.967	9.781	4.793	9.873
3.118	9.772	4.908	9.889
3.197	9.793	4.950	9.891
3.472	9.791	5.188	9.922
3.602	9.802	5.363	9.928
3.713	9.801	5.576	9.956
3.848	9.812	5.577	9.954
4.541	9.867	5.716	9.984
4.549	9.851	5.888	10.00
4.553	9.859		

where

$$W_0 = \rho_0/L_0T \tag{3}$$

$$W_{ep} + W_d = (\rho_{ep} + \rho_d)/L_0T \tag{4}$$

$$W_{ee} = \rho_{ee}/L_{ee}T \tag{5}$$

W_v is the component of the thermal resistivity due to inelastic electron–phonon scattering (vertical processes on the Fermi surface), W_m is the component of the thermal resistivity due to the scattering of electrons by magnetic impurities, ρ_0 is the temperature-independent residual resistivity due to impurities and physical imperfections, ρ_{ep} is the resistivity due to electron–phonon scattering, ρ_d represents deviation from Matthiessen's rule (DMR), ρ_{ee} is due to electron–electron scattering, ρ_m is the Kondo component due to the scattering of electrons by magnetic impurities, $L_0 = 2.443 \times 10^{-8}$ W Ω K^{-2} is the Sommerfeld value of the Lorenz number and L_{ee} is the number which corresponds to L_0 for electron–electron scattering.

3.1. Methods of analysis

In the past an analysis of electrical resistivity data required an extrapoltation of ρ to $T = 0$ to obtain ρ_0. In this method one assumed, with guidance from theoretical models, that the resistivity could be expressed by an equation of given form, for example by an equation

$$\rho = \rho_0 + aT^2 + bT^5. \tag{6}$$

This equation was put in the form

$$(\rho - \rho_0)/T^2 = a + bT^3$$

and $(\rho - \rho_0)/T^2$ was plotted as a function of T^3 to obtain a linear graph with slope b and y intercept a which determined the values of the constants a and b.

More recently the method outlined by Ribot *et al* [5] has been used. This also requires that one assumes the form of an equation such as equation (6). One then takes the derivative of this equation with respect to T and divides by T to obtain

$$(1/T)\,\mathrm{d}\rho/\mathrm{d}T = 2a + 5bT^3.$$

If $d\rho/dT$ is replaced by the experimentally determined values $\Delta\rho/\Delta T$, then plots of $(1/T)\,\Delta\rho/\Delta T$ as a function of T^3 produce a linear graph in which $5b$ is the slope and $2a$ is the y intercept, and hence a and b are determined. This method has the advantage that the value of ρ_0 is not required and therefore errors due to imperfect extrapolations of ρ to ρ_0 at $T = 0$ do not affect the values of a and b.

In this work we employ multiple linear regression analysis (MLRA) to fit experimental data to an assumed equation such as equation (6). In this case one may think of ρ_0 as an adjustable parameter, which merely raises or lowers the curve (represented by $aT^2 + bT^5$) parallel to the y axis without affecting either the shape of the curve or the values of a and b obtained by carrying out the curve fit to the data points. It therefore has the same advantage as the previous method as well as several other advantages. It can be applied to equations which cannot be linearized. The values of all parameters, including ρ_0, and their error estimates are easily obtained. If high-accuracy data are available the accuracy of the parameters is not limited by how well the slope and intercept can be read on graph paper. If the exact form of the trial equation is not known, for example, if it is not known that the third term in equation (6) varies as T^5, then an equation of the form

$$\rho = \rho_0 + aT^2 + bT^n$$

may be fitted to determine n. However, in this case it is necessary to determine four parameters and unless adequate data are available a fit may not be obtained or it may be obtained with large estimated standard deviations in the parameters ρ_0, a, b and n.

In MLRA an estimate of the required parameters is input into the computer and the program varies these parameters to converge on values which give the best fit. If the combination of accuracy, number of available data points and ranges of the independent and dependent variables is inadequate for the number of parameters that must be determined, convergence does not occur and the values of the required parameters cannot be obtained.

We also use least-mean-squares fits (LMSF) to a polynomial such as

$$y = a + bx + cx^2 + \ldots + nx^m.$$

Fits to equations of the type

$$y = a + b \ln T$$

or

$$y = a + bT^2$$

can be obtained by setting $x = \ln T$ or $x = T^2$ and fitting

$$y = a + bx$$

to the data $(y, \ln T)$ or (y, T^2). A fit is always obtained regardless of the quality of data. For poor data the errors in the coefficients may be considerably larger than the coefficients themselves, therefore the estimated errors in the coefficients must always be calculated to determine whether the fit provides meaningful values of the coefficients. It is customary to omit points that are more than two standard deviations from the curve; however, the number of points removed must be small relative to the total number available for a fit in a given range.

Table 4. Coefficients obtained by MLRA to equation (6) for $T > 2.85$ K. Average value $\langle a \rangle$ of a for R data, $\langle a \rangle = (4.14 \pm 0.44) \times 10^{-15}$ Ω m K^{-2}.

Sample	ρ_0 (10^{-12} Ω m)	a (10^{-15} Ω m K^{-2})	b (10^{-17} Ω m K^{-5})
Al-1	9.7314 ± 0.0070	4.61 ± 0.61	1.58 ± 0.24
RAl-1	0.9211 ± 0.0004	4.24 ± 0.05	1.42 ± 0.04
RAl-2	0.659 ± 0.002	4.5 ± 0.2	1.1 ± 0.2
RAl-3	1.2919 ± 0.0004	4.74 ± 0.05	1.67 ± 0.04
RAl-4	2.9103 ± 0.0004	4.77 ± 0.05	2.33 ± 0.04
RAl-5	106.792 ± 0.001	3.6 ± 0.2	4.6 ± 0.1
RAl-6	110.627 ± 0.002	4.2 ± 0.2	4.2 ± 0.2
RAl-7	6.6195 ± 0.0006	3.65 ± 0.09	2.72 ± 0.08
RAl-8	5.998 ± 0.002	3.9 ± 0.2	2.4 ± 0.2
RAl-9	22.4413 ± 0.0002	3.75 ± 0.03	2.41 ± 0.03

3.2. Analysis of electrical resistivity data

The data used are listed in table 3 and also in the appendix of [5], which provides a large amount of very high-quality data, which we will refer to as R data. To present the most logical account of our results we begin with the analysis of the resistivity data referred to above. In practice, we actually began with the analysis of only our own data along the lines described in section 3.3 below and arrived at a graph similar to that of figure 5. At that stage, it was suspected that points below 2.85 K included an additional electron-scattering term, which decayed rapidly with increasing temperature and whose effect above 2.85 K was negligible. If this were the case, it was surmised that the effects of the same scattering process should also appear in the electrical resistivity. A search of the literature revealed the R data presented in figure 10 of [5], which indicated that between 2.85 K and 4.2 K the points for a given sample fall on a straight line and that a definite kink occurs at about 2.85 K.

Fits of the R data between 2.85 K and 4.2 K to equation (6) were carried out using MLRA to determine ρ_0, a and b for each of the nine samples. A similar fit was carried out for data obtained for sample Al-1 from 2.9 K to 5.9 K. These fits were excellent. Most points fitted the curve to better than one part in 10^3. The values of the parameters ρ_0, a and b and their estimated standard deviations are listed in table 4. It is noted that the values of a for the R data are approximately equal, though not within their calculated error limits, and that the average value $\langle a \rangle = (4.14 \pm 0.44) \times 10^{-15}$ Ω m K^{-2} is, within error limits, equal to $a = (4.6 \pm 0.6) \times 10^{-15}$ Ω m K^{-2} for sample Al-1. A visual presentation of these results is provided in figure 1, where equation (6) is written in the form

$$(\rho - \rho_0)/T^2 = a + bT^3$$

and $(\rho - \rho_0)/T^2$ is plotted as a function of T^3 for samples RAl-1–RAl-4 (the value of ρ_0 used is that obtained by MLRA). In the absence of an additional scattering process below 2.85 K equation (6) could be extrapolated to $T = 0$ (broken lines). The additional effect therefore manifests itself in the rise of data points above the broken lines. Similar results were obtained for the remaining samples with the exception of RAl-5 and RAl-9, where the extraneous effects were about five times smaller in RAl-5 and two times smaller in RAl-9. Clearly, an additional term ρ_m must be added to equation (6) and its magnitude as a function of temperature can be determined from

$$\rho_m = \rho - (\rho_0 + aT^2 + bT^5).$$

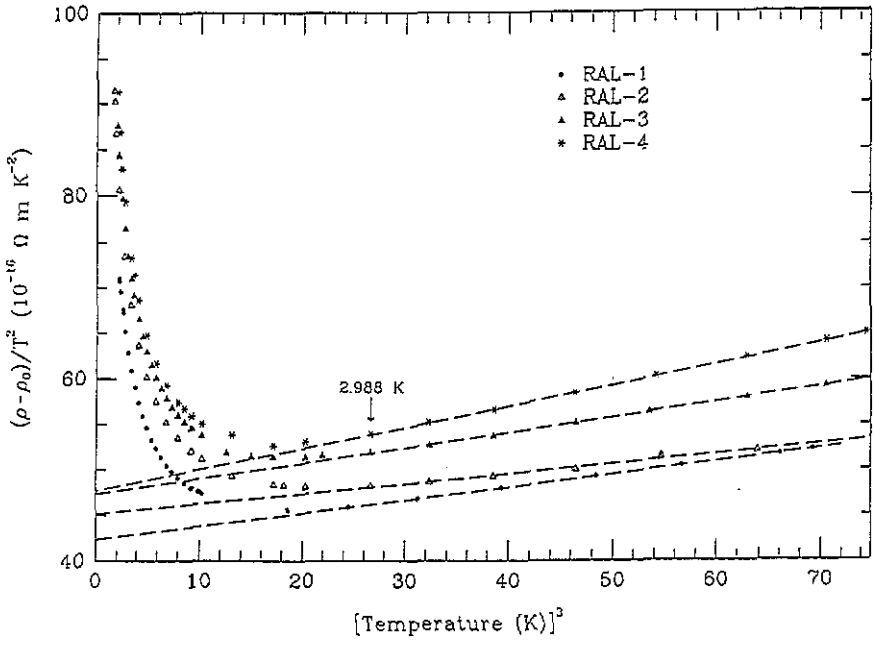

Figure 1. Graphs of $(\rho - \rho_0)/T^2$ versus T^3 as a visual representation of the fits obtained to equation (6) using MLRA to data between 2.85 K and 4.2 K.

It is known that magnetic impurity scattering produces a component

$$\rho_m = c(1 + d \ln T) \qquad \text{for } T > T_K$$

and

$$\rho_m = e[1 - (T/\theta)^2] \qquad \text{for } T < T_K$$

where T_K is the Kondo temperature. To determine whether ρ_m could be attributed to magnetic impurity scattering the (ρ_m, T) data were fitted to the equation

$$\rho_m = \alpha + \beta \ln T \qquad (1.6 \text{ K} < T < 2.9 \text{ K}) \tag{7}$$

for all nine samples, RAl-1–RAl-9. When points below 1.6 K were omitted good fits were obtained, as shown in figure 2 for samples RAl-1 to RAl-4. The values and estimated standard deviations of the coefficients of equation (7) for all nine samples and the points used (starting with point No 1 at the lowest temperatures—as listed in reference [5]) are given in table 5. It is noted that for all samples $\alpha \simeq \beta$, though not within the estimated standard deviations of α and β.

For samples RAl-1 to RAl-4 and RAl-7 points below 1.6 K provided a good LMSF to an equation of the form

$$\rho_m = \gamma - \delta T^2 \qquad (T < 1.6 \text{ K}). \tag{8}$$

In the remaining four samples the number of points below 1.6 K was insufficient to provide meaningful fits. Values of the coefficients of equation (8), their estimated standard deviations

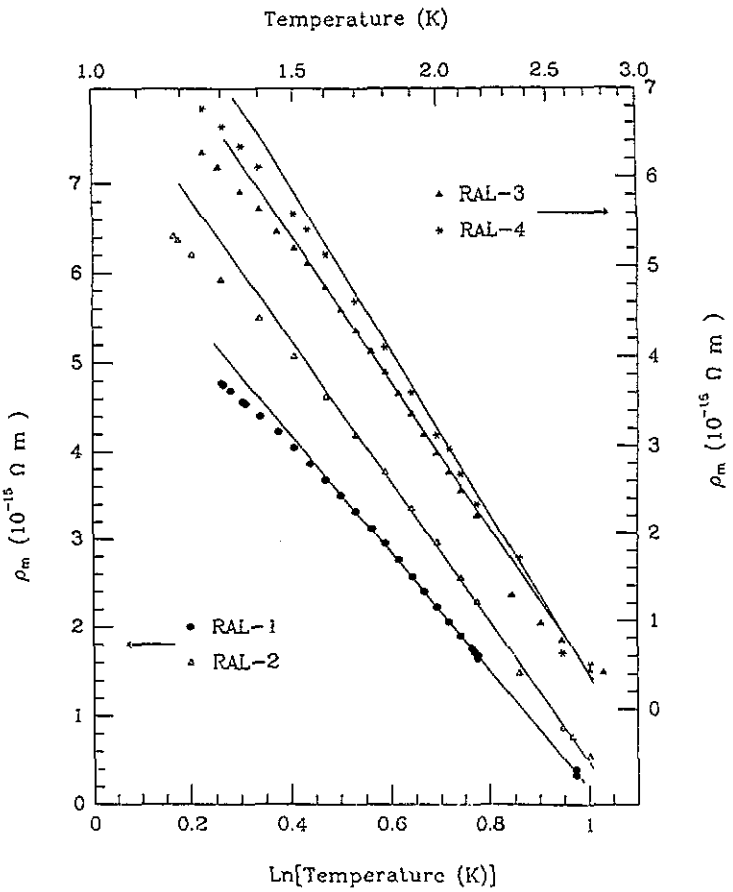

Figure 2. Graphs of ρ_m versus $\ln T$ for 1.6 K < T < 2.85 K.

Table 5. Coefficients obtained by MLRA to equation (7).

Sample	Temperature range (K)	Points used	α (10^{-15} Ω m)	β (10^{-15}) in SI units
RAI-1	1.70–2.65	Nos 15–31, 33	6.93 ± 0.01	6.78 ± 0.01
RAI-2	1.70–2.73	Nos 8–13, 15–17	8.40 ± 0.04	7.88 ± 0.05
RAI-3	1.65–2.73	Nos 10–20, 22–24	8.74 ± 0.06	8.41 ± 0.08
RAI-4	1.54–2.73	Nos 6–15, 17	9.21 ± 0.05	8.74 ± 0.07
RAI-5	1.52–2.16	Nos 1–4	2.37 ± 0.04	2.34 ± 0.06
RAI-6	1.77–2.61	Nos 3–6	8.8 ± 0.2	8.8 ± 0.3
RAI-7	1.60–2.63	Nos 4–9	4.39 ± 0.01	4.46 ± 0.02
RAI-8	1.66–2.61	Nos 2–5	5.55 ± 0.02	5.54 ± 0.03
RAI-9	1.76–2.62	Nos 3–6	2.96 ± 0.03	3.04 ± 0.03

and the values of $\theta = (\gamma/\delta)^{1/2}$ are listed in table 6 and graphs for samples RAI-1 to RAI-4 are illustrated in figure 3.

The above analysis provides convincing evidence for the existence of magnetic impurity scattering (with a Kondo temperature $T_K \approx 1.6$ K) in the R data. Unfortunately, an impurity analysis for these samples is not available and the magnetic impurity causing the scattering

Table 6. Coefficients obtained by MLRA to equation (8). Average value $\langle\theta\rangle$ of θ for R data, $\langle\theta\rangle = (2.361 \pm 0.026)$ K.

Sample	γ (10^{-15} Ω m)	δ (10^{-15} Ω m K^{-2})	$\theta = (\gamma/\delta)^{1/2}$ (K)
RAl-1	6.86 ± 0.02	1.234 ± 0.008	2.358 ± 0.008
RAl-2	8.51 ± 0.04	1.53 ± 0.02	2.36 ± 0.01
RAl-3	8.61 ± 0.02	1.51 ± 0.01	2.388 ± 0.005
RAl-4	9.36 ± 0.03	1.65 ± 0.01	2.381 ± 0.005
RAl-7	4.391 ± 0.002	0.819 ± 0.008	2.32 ± 0.01

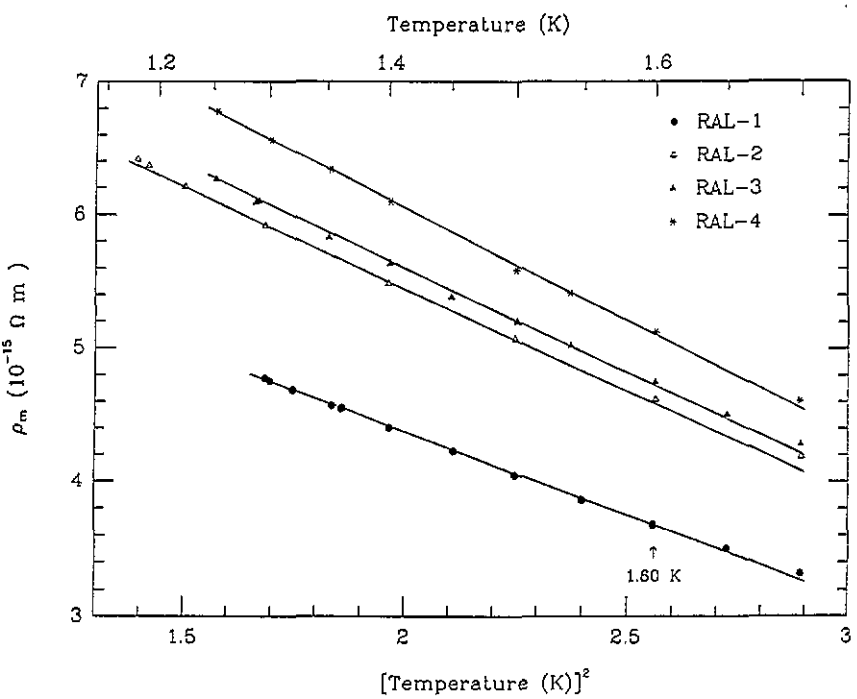

Figure 3. Graphs of ρ_m versus T^2 for $T < 1.6$ K.

cannot be identified. It is surprising that the samples vary by more than two orders of magnitude in ρ_0, but ρ_m is approximately equal for all samples except RAl-5 and RAl-9. Since the latter is unannealed and impurities in Al tend to aggregate along dislocations and grain boundaries, the effect of magnetic impurities is expected to be relatively reduced in this sample.

If it is accepted that the R data contain a term due to an extraneous scattering process then the data below 2.85 K must be omitted to properly determine the other terms in equation (2). In this case the aT^2 term of equation (6) may be identified with electron–electron scattering. The fact that it has nearly the same magnitude for all samples supports this contention. Moreover, the values of the coefficients a ($\langle a\rangle = (4.14 \pm 0.44) \times 10^{-15}$ Ω m K^{-2} for the R data and $a = (4.6 \pm 0.6) \times 10^{-15}$ Ω m K^{-2} for Al-1) agree well with the value $a_{calc} = 4.1 \times 10^{-15}$ Ω m K^{-2} determined by MacDonald [9]. On the other hand the magnitude of the bT^5 term varies with ρ_0 and therefore cannot be identified with electron–phonon scattering (ρ_{ep}).

In figure 4, b is plotted as a function of log ρ_0. A linear relationship is obtained for all annealed samples (Al-1 and RAl-9 are unannealed). The plus sign for Al-2 does not represent a data point, rather it indicates the value of b expected for our annealed sample Al-2 on the basis of the value of ρ_0 determined for Al-2. An LMSF of the (b, ρ_0) data to the equation

$$b = f + g(\log \rho_0) \tag{9}$$

yields values $f = (1.99 \pm 0.06) \times 10^{-16}$ Ω m K^{-5} and $g = (1.53 \pm 0.05) \times 10^{-18}$ SI units. Therefore, the bT^5 term can be resolved into two components, fT^5 and $g(\log \rho_0)T^5$. Since the former is independent of ρ_0 we attribute it to electron–phonon scattering (ρ_{ep}) and we attribute the latter to DMR (ρ_d). The latter form is consistent with the theoretical work of Bergman *et al* [11] and Kaveh and Wiser [12].

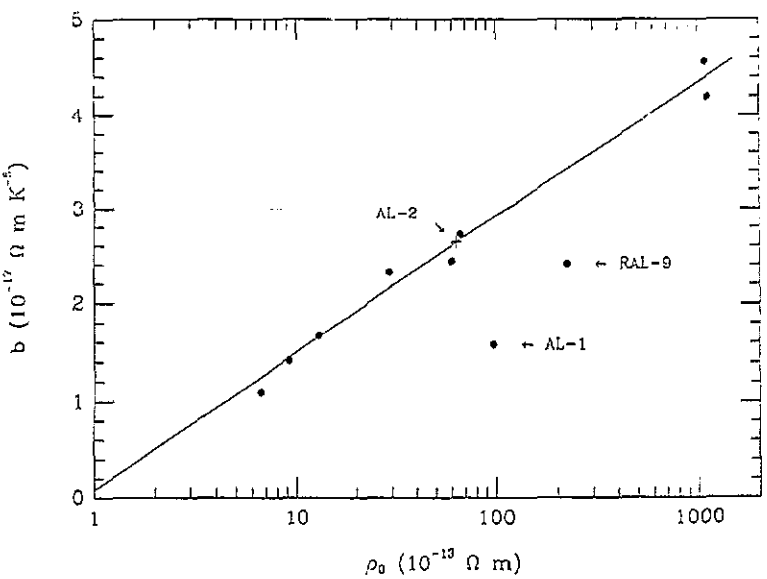

Figure 4. Graph of b versus log ρ_0 for annealed samples (Al-1 and RAl-9 are unannealed).

3.3. Analysis of thermal resistivity data

If the last five terms in equation (1) are relatively small compared to W_0, then at sufficiently low temperatures an approximate value L_0^E (experimentaly determined value of L_0) may be found from a linear fit of the thermal conductivity data K_c as a function of T where the line is forced to pass through the origin ($K_c = 0$, $T = 0$). In our case the required condition is not fulfilled, therefore an alternative method for determining L_0 is employed.

Equation (1) (with $W_m = 0$) is written as

$$(W - W_{ep} - W_d)T = \rho_0/L_0^E + (W_{ee} + W_v)T \tag{10}$$

where $(W_{ep} + W_d) = (\rho_{ee} + \rho_d)/L_0'T$, $(\rho_{ep} + \rho_d) = bT^5$, and the value of L_0' is assumed to be equal to the Sommerfeld value L_0. If this assumption is not well satisfied, the error

introduced will not be large because $W_{ep} + W_d$ is small compared to W (less than 0.3% at 3 K and less than 0.5% at 4 K). The value b for Al-1 was found from our resistivity data as listed in table 4 and for Al-2 it was determined to be 2.4×10^{-17} Ω m K^{-5} from equation (9) as shown in figure 4. Equation (10) can be written in the form

$$Z = C + AT^J + BT^K$$

where $Z = (W - W_{ep} - W_d)T$, $C = \rho_0/L_0^E$, $A = W_{ee}/T^{J-1}$ and $B = W_v/T^{K-1}$, then using MLRA a fit of data from 2.85 K to 4.0 K was attempted to provide values of C, A, B, J and K. Unfortunately, the data are not sufficiently good for convergence to occur. Even when J is set equal to two (it is assumed that $W_{ee} = AT$) the data are still inadequate to determine the remaining four parameters.

A fit of data between 2.85 K and 4 K was carried out to the equation

$$Z = C + DT^M \tag{11}$$

where $Z = (W - W_{ep} - W_d)T$, $C = \rho_0/L_0^E$ and $DT^M = (W_{ee} + W_v)T$. The parameters C, D and M and their estimated standard deviations are listed in table 7, as are the calculated values of L_0^E. It is encouraging that these values are, within the error limits, equal to the Sommerfeld value of L_0; consequently, in subsequent calculations we will use $L_0^E = L_0' = L_0 = 2.443 \times 10^{-8}$ W Ω K^{-2}. Since $L_0 = \pi^2 k^2/3e^2$ is a fundamental constant all good data, properly analysed, should yield this value for all metals in the limit $T \to 0$. Graphs of Z as a function of T^M for Al-1 and Al-2 are presented in figure 5. They also include data points below 2.85 K which indicate the existence of an extraneous scattering process. It is unlikely that this anomaly is due to thermometry errors or a fault of the apparatus because recent measurements on free hanging samples of potassium using the same apparatus do not show any anomalies between 2 K and 3 K. Since the effect decays as the temperature is increased, becoming negligible at 2.85 K, it is reasonable to attribute it to magnetic impurity scattering of the same type as observed in the R data.

Table 7. Parameters C, D and M from an MLRA fit of data to equation (11), calculated value of L_0^E and parameters A, E and N from an MLRA fit of data to equation (12).

Parameter	Al-1	Al-2
C (10^{-4} m K^2 W^{-1})	3.969 ± 0.011	2.585 ± 0.008
D (10^{-7} SI units)	1.74 ± 0.61	1.42 ± 0.43
M	3.71 ± 0.23	3.73 ± 0.20
L_0^E (10^{-8} W Ω K^{-2})	2.45 ± 0.01	2.44 ± 0.03
A (10^{-7} m W^{-1})	3.6 ± 2.3	6.85 ± 0.62
E (10^{-9} SI units)	24 ± 28	2.25 ± 2.05
N	2.99 ± 0.75	4.41 ± 0.64

Equation (1) may now be written as:

$$(W - W_{ep} - W_d - W_0)/T = W_{ee}/T + W_v/T$$

which has the form

$$Y = A + ET^N \tag{12}$$

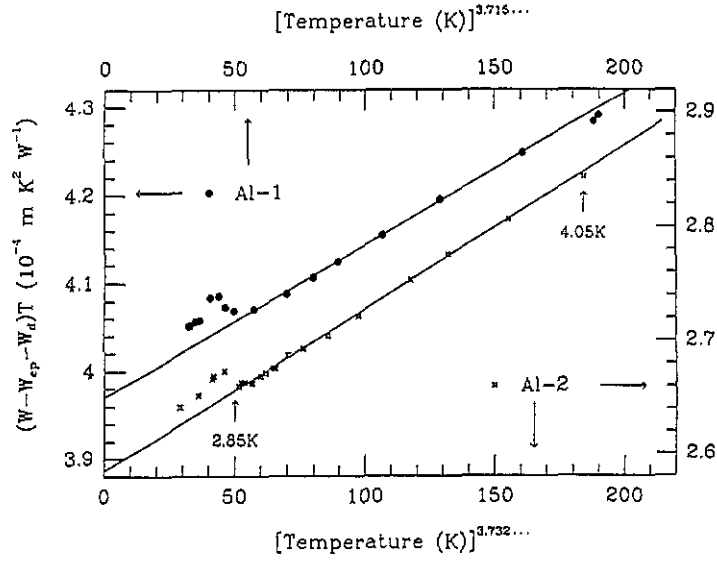

Figure 5. Graphs of $(W - W_{ep} - W_d)T$ versus $T^{3.715...}$ for Al-1 and versus $T^{3.732...}$ for Al-2 (the intercepts determine $C = \rho_0/L_0^E$).

where $Y = (W - W_{ep} - W_d - W_0)/T$, $A = W_{ee}/T$ and $E = W_v/T^{N+1}$. A fit of Y as a function of T^N for 4.0 K > T > 2.85 K yields the parameters listed in table 7. Graphs of these fits are presented in figure 6, where the scales along the x and y axes are different for each sample and where data below 2.85 K are included. These graphs are somewhat misleading as they appear to indicate that the y intercepts and slopes are well determined. However, these graphs are plotted for a fixed value of N, as if it were known exactly, whereas the values of all three parameters A, E and N were determined concurrently, and are uncertain within the calculated error limits. The standard deviations listed in table 7 are correct and unfortunately quite large. For sample Al-1, only six points are available for the fit and the value of A is poorly determined. For Al-2, 14 points are available and the value of A is reasonably well determined (to within 5%), and is in good agreement with the theoretical value provided by MacDonald [9].

The data below 2.85 K are similar for both samples. To obtain a better appreciation of the form and magnitude of this anomaly values represented by equation (12) were multiplied by T, then subtracted (along with W_{ep}, W_d and W_0) from values of the measured thermal resistivity to give

$$W_m = W - (W_{ep} + W_d + W_0 + AT + ET^{N+1})$$

as shown in figure 7. For both samples the effect increases rapidly from 2.85 K with decreasing temperature, reaching a maximum at 2.7 K, and subsequently decreases. The magnitude of the rise is almost twice as large for sample Al-1 as for Al-2. Insufficient data are available for a proper analysis of data for Al-2, but the values of W_m for the five points representing the rise of the data for Al-1 are plotted as a function of $\ln T$ in figure 8. An LMSF of these data to an equation of the form

$$W_m = P - Q \ln T \tag{13}$$

provided the following values and estimated standard deviations of the coefficients: $P = (1.82 \pm 0.28) \times 10^{-5}$ m K W^{-1}; $Q = (1.68 \pm 0.27) \times 10^{-5}$ SI units.

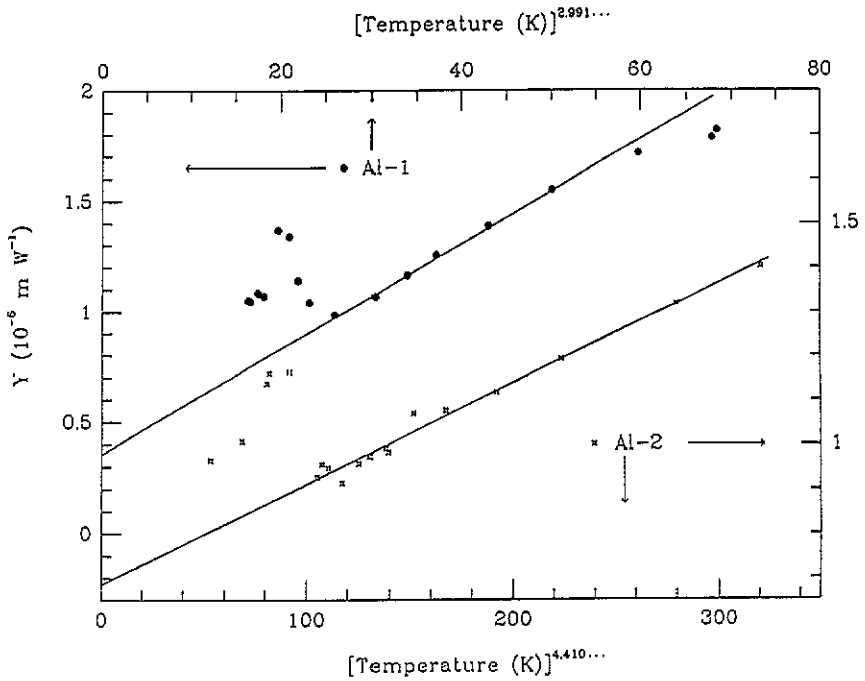

Figure 6. Graphs of $(W - W_{ep} - W_d - W_0)/T$ versus $T^{2.991...}$ for Al-1 and versus $T^{4.410...}$ for Al-2 (the intercepts determine $A = W_{ee}/T$).

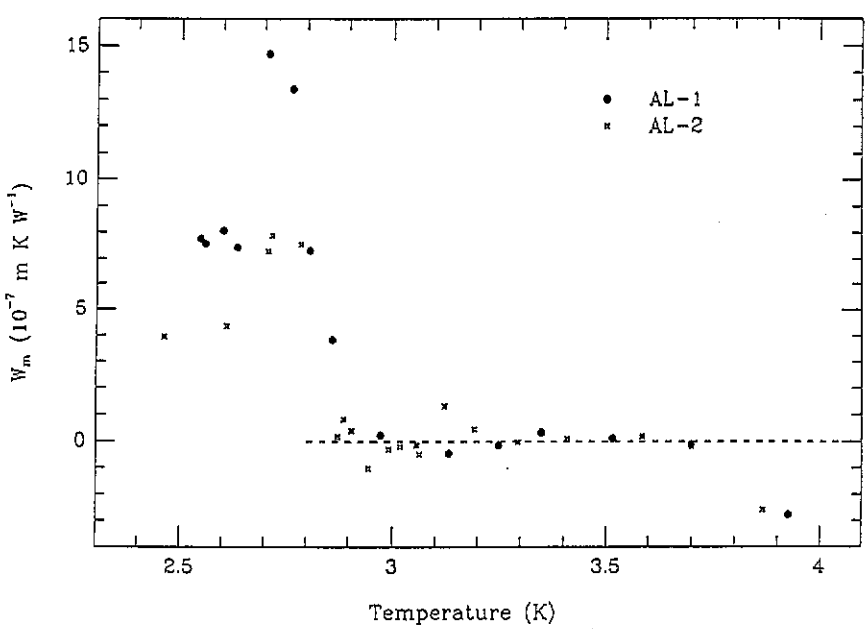

Figure 7. Graphs of $W_m = W - (W_{ep} + W_d + W_0 + AT + ET^{N+1})$ versus T for Al-1 and Al-2.

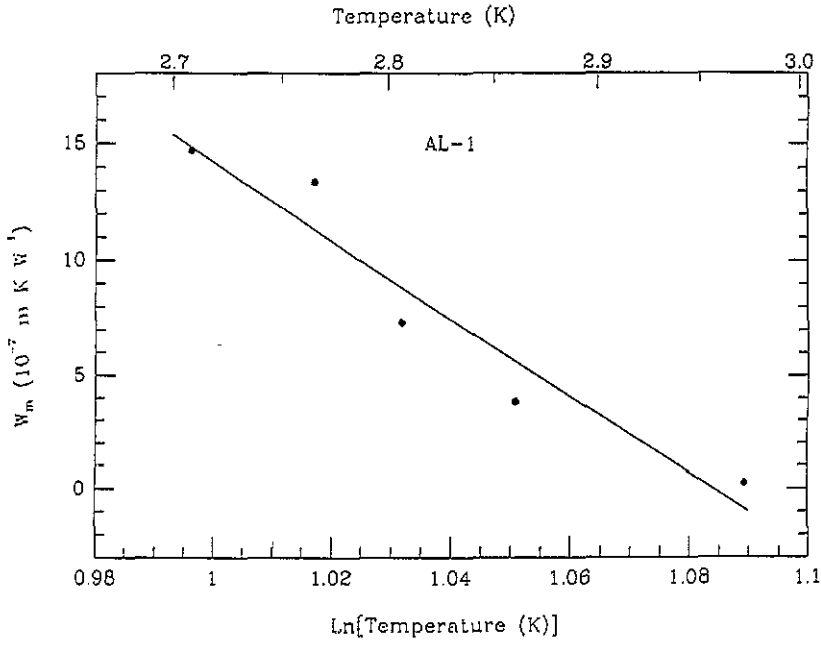

Figure 8. Graph of W_m versus ln T for Al-1.

4. Conclusion and discussion

The analysis of our data and the R data provides excellent support for the theoretical work of MacDonald [9] on electron–electron scattering in Al. A comparison of the relevant theoretical and corresponding experimental values is provided in table 8. All experimental values are in good agreement with theory with the exception of W_{ee}/T for Al-1. In this case the estimated standard deviation is sufficiently high as to cast considerable doubt on this value.

Values of L_0^E, $\rho_{ee}/T^2 = \langle a \rangle$ and ρ_{ep}/T^5 were obtained to better than 1% of the theoretical values, although in the latter case the agreement may be fortuitous because the uncertainty in the extrapolation to obtain the theoretical value is likely to be considerably larger than 1%.

Unfortunately, the available data do not allow a calculation of L_{ee} from data obtained on a single sample. The two experimentally obtained values of L_{ee} were calculated by dividing ρ_{ee}/T^2 (from R data) and ρ_{ee}/T^2 (from Al-1 data) by W_{ee}/T (from Al-2 data).

Values of ρ_{ee}/T^2 vary considerably, from 3.55×10^{-15} Ω m K^{-2} (for RAl-5) to 4.77×10^{-15} Ω m K^{-2} (for RAl-4) with no apparent correlation to ρ_0 or any other parameter. (The variation is much larger than expected from the error estimates, which indicate, for example, that ρ_{ee}/T^2 for RAl-4 has a minimum value of 4.715×10^{-15} Ω m K^{-2} while for RAl-5 it has a maximum value of 3.71×10^{-15} Ω m K^{-2}.) This result is particularly surprising for the unannealed sample RAl-9. Kaveh and Wiser [13] showed that ρ_{ee}/T^2 is a monotonically increasing function of the relative dislocation density (ρ_{0d}/ρ_{0i}) where ρ_{0i} is the electron–impurity component of ρ_0 and $\rho_{0d} = \rho_0 - \rho_{0i}$. Although the maximum increase for Al is estimated to be about 25% it is clear from figure 4 that the dislocation density in RAl-9 is not insubstantial, yet its ρ_{ee}/T^2 is one of the smaller values in the list and within error estimates considerably smaller than the average.

Table 8. A comparison of theoretical and experimental values of ρ_{ep}/T^5, L_0, ρ_{ee}/T^2 and W_{ee}/T.

	ρ_{ep}/T^5 (10^{-16} Ω m K^{-5})	L_0 (10^{-8} W Ω m K^{-2})	ρ_{ee}/T^2 (10^{-15} Ω m K^{-2})	W_{ee}/T (10^{-7} m W^{-1})	L_{ee} (10^{-9} W Ω K^{-2})
Theoretical	2.0	2.443	4.1	7.1	5.8
Experimental (R data)	1.99 ± 0.06	—	4.14 ± 0.44	—	6.1 ± 1.3
Al-1	—	2.452 ± 0.009	4.6 ± 0.6	3.6 ± 2.3	6.8 ± 1.9
Al-2	—	2.44 ± 0.02	—	6.8 ± 0.6	—

It is important to note, as clearly explained by Kaveh and Wiser [6], that in Al both ρ_{ee}/T^2 and W_{ee}/T are functions of temperature. They are reasonably constant only below 4.2 K but decrease by nearly an order of magnitude from 4.2 K to 42 K. However L_{ee} remains approximately constant.

The value $f = \rho_{ep}/T^5$ obtained from equation (9) is in good agreement with the value of f determined by extrapolating the theoretical results of Lawrence and Wilkins [4] below 3 K. On the other hand, the experimental results suggest that f remains a constant and that the T^5 dependence persists up to at least 4.2 K, and therefore disagree with the theoretical work [4], which indicates that above 3 K the power to which T is raised decreases toward a value of 'roughly four' as the temperature is raised toward 10 K. It is surprising to find the ρ_{ep} and ρ_d terms combined in the form of equation (9) where the second term is negative for $\rho_0 < 1$. (This form is similar to equation (7), with T replaced by ρ_0.) As ρ_0 is decreased the magnitude of $g \log \rho_0$ increases, reducing the value of b. However, a limit to this effect must exist. If equation (9) is extrapolated to $\rho_0 < 10^{-13}$ Ω m it predicts negative values for b—an unphysical result!!

All values in table 8 were obtained by omitting points below 2.85 K and therefore are independent of the nature of the extraneous scattering process. However, substantial evidence was provided to suggest that the extraneous resistivity is due to magnetic impurity scattering (with $T_K \simeq 1.6$ K), and it is reasonable to suggest that the same impurity also produces the observed extraneous thermal resistivity in samples Al-1 and Al-2. In a table of characteristic temperatures (table 2) Rossiter [14] lists only Cr and Mn as known impurities producing Kondo scattering in Al. These however are reported to have values of $T_K \simeq 1200$ K and 530 K respectively [15]. In [15] measurable effects were produced with concentrations of 900–10^4 ppm Cr and 480–5×10^4 ppm Mn. The impurity analyses for Al-1 and Al-2 quote concentrations of 5 ppm and 6 ppm of Mn respectively, which on the basis of [15] would result in effects too small to be observed. With the information available it is not possible to identify the impurity giving rise to the extraneous resistivities in our samples and in the R data.

The form of the extraneous thermal resistivity detected in Al-1 and Al-2 is not well determined because too few points are available in the temperature range of interest. The LMSF to equation (13) does not provide a sufficiently convincing graph (figure 8) to determine that W_m varies as $\ln T$. However, it is clear from figure 7 that the general behaviour of W_m as a function of T is similar in both samples, that a maximum is reached at 2.7 K and that a subsequent decrease with decreasing T occurs to an approximately level value between 2.65 K and 2.5 K. The level value is about 4×10^{-7} m K W^{-1} for Al-2 and 8×10^{-7} m K W^{-1} for Al-1 and the ratio of the peaks is in about the same proportion. It is also certain that the functional relation between W_m and T is quite different from that between ρ_m and T, where there is a monotonic increase in ρ_m with decreasing T for all samples to the lowest temperatures measured ($T \simeq 1.25$ K).

In this paper it is shown that if thermal resistivity data are neglected below 2.85 K, then values between 2.85 K and 4 K may be extrapolated to obtain the Sommerfeld value of L_0 to within about 1% for both samples Al-1 and Al-2. In addition, this procedure allows the determination of W_{ee}/T for sample Al-2 to within 5% of the theoretical value calculated by MacDonald [9]. The anomaly detected below 2.85 K in both samples is to some extent confirmed by the anomaly that appears in the R data at 2.85 K (figure 10 of [5]).

Ribot *et al* [5] proposed the following explanation for this anomaly: 'If this model is correct, then as the temperature is raised above T_λ (≈ 2.2 K), $\rho(T)$ should increase less rapidly than T^5, and the resistivities of the purer samples should fall below those of the less pure samples as the purer samples move out of the dirty limit'. This explanation is

questionable on two counts. First, it is surprising that all samples would 'move out of the dirty limit' over the narrow temperature range 2.2–2.85 K when their values of ρ_0 vary substantially, the largest being 160 times the smallest. Second, it is not the power of the T^5 term that changes as the temperature is increased; rather the coefficients of the T^2 and T^5 terms change according to figure 10 of [5] and our analysis. We therefore disagree with the claim of Ribot *et al* regarding the observed temperature dependence above 2.2 K.

An alternative explanation of the R data is presented in which it is assumed that the observed anomalies in the thermal and electrical resistivities below 2.85 K are due to the occurrence of an additional electron-scattering process. In this case only data above 2.85 K may be used to determine ρ_{ee}, ρ_{ep} and ρ_d. An analysis of our resistivity data and of the R data shows that equation (6) provides an excellent fit to all samples above 2.85 K and that the T^5 variation, as a component of this equation, continues to at least 4.2 K for all samples. This result is confirmed by the analysis of Ribot *et al* (figure 10 of [5]). When straight lines are drawn through the data above 2.85 K on an enlarged copy of their figure 10, the slopes and intercepts provide essentially the same values of a and b as our MLRA fits of these data to equation (6).

In our interpretation of the R data the average value of a is within 1% of the theoretical value calculated by MacDonald [9] and the values of b plotted as a function of ρ_0 (figure 4) allow a separation of the bT^5 term into two components. One component is independent of ρ_0 and may be associated with ρ_{ep}, while the other, ρ_d, represents DMR. The value of ρ_{ep} obtained in this manner agrees with the value obtained by extrapolating the results of the Lawrence and Wilkins model (which does not take into account DMR) to low temperatures.

In the interpretation presented the excess resistivity ρ_m (above the values obtained by extrapolating equation (6) to temperatures below 2.85 K) is due to an additional scattering process. Remarkably, the temperature variation of ρ_m is exactly that which is expected for Kondo scattering with $T_K \simeq 1.6$ K, though insufficient information is available to associate this effect with a determined impurity.

It is, of course, possible that some of the excellent agreement between theory and experiment is fortuitous and any one of the results obtained in our interpretation of the R data may be attributed to coincidence. However, all the results presented, taken together, lend a degree of confidence in and justification for our interpretation of the R data.

Acknowledgments

The authors wish to acknowledge their debt to Dr R Barton for many valuable discussions and his generous help with computer programming. We thank Mr D Kolybaba for very professional machine-shop services, Mr B Ramadan, Mr K Wolbaum and Mr D Janz for their excellent electronics services. One of us (YH) is grateful for the award of a Saskatchewan Graduate Student Scholarship and a Teaching Assistantship from the University of Regina.

References

[1] Bass J, Pratt W P Jr and Schroeder P A 1990 *Rev. Mod. Phys.* **62** 645–744
[2] Garland J C and Bowers R 1969 *Phys. Kondens. Mater.* **9** 36
[3] Lawrence W E and Wilkins J W 1973 *Phys. Rev.* B **7** 2317–32
[4] Lawrence W E and Wilkins J W 1972 *Phys. Rev.* B **6** 4466–82
[5] Ribot J H J M, Bass J, van Kempen H, van Vucht R J M and Wyder P 1981 *Phys. Rev.* B **23** 532–51
[6] Kaveh M and Wiser N 1984 *Adv. Phys.* **33** 257–372

[7] van Wucht R J M, van Kempen H and Wyder P 1985 *Rep. Prog. Phys.* **48** 853–905
[8] MacDonald A H and Geldart D J W 1980 *J. Phys. F: Met. Phys.* **10** 677–92
[9] MacDonald A H 1980 *Phys. Rev. Lett.* **44** 489–93
[10] Kos J F 1990 *J. Phys.: Condens. Matter* **2** 4859–68
[11] Bergman Y, Kaveh M and Wiser N 1974 *Phys. Rev. Lett.* **32** 606–9
[12] Kaveh M and Wiser N 1980 *Phys. Rev.* B **21** 2291–308
[13] Kaveh M and Wiser N 1980 *J. Phys. F: Met. Phys.* **10** L37–42
[14] Rossiter P L 1986 *Aust. J. Phys.* **39** 529–45
[15] Caplin A D and Rizzuto C 1968 *Phys. Rev. Lett.* **21** 746–8
[16] *Handbook of Chemistry and Physics* 1975 55th edn (Cleveland, OH: Chemical Rubber Company) p B-5